Third harmonic generation of CO_2 laser radiation in $AgGaSe_2$ crystal

GOPAL C BHAR, PATHIK KUMBHAKAR[1], D V SATYANARAYANA[2],
N S N BANERJEE[2], U NUNDY[2] and C G CHAO[3]

Laser Laboratory, Physics Department, Burdwan University, Burdwan 713 104, India
[1] Present address: Physics Department, Regional Engineering College, Durgapur 713 209, India
[2] Centre for Advanced Technology, Indore 452 013, India
[3] Anhui Institute of Optics and Fine Mechanics, China
Email: buphygcb@dte.vsnl.net.in

Abstract. Generation of third harmonic of CO_2 laser radiation has been obtained in a type-II, $\theta = 57°$ cut 9 mm thick $AgGaSe_2$ crystal for the first time by sum-frequency-mixing of the fundamental with its second harmonic, the latter being obtained using another type-I, $\theta = 55°$ cut 11 mm thick $AgGaSe_2$ crystal. The energy conversion efficiencies obtained for second harmonic and third harmonic generations are 6.3% and 2.4% respectively with the input fundamental pump power density of 5.9 MW/cm^2 only. The wavelength of the fundamental CO_2 laser radiation used for the generation of harmonics is 10.6 μm, $P(20)$ line. A compact TEA CO_2 laser source has been built in the laboratory.

1. Introduction

Mid infrared (MIR) region 2–5 μm of the atmospheric window is important as it carries the finger prints of the atmospheric trace constituents. There are several reports of generation of radiation in the above region by difference frequency mixing in different NIR (near infrared) non-linear crystals. But the use of all these sources is limited by low conversion efficiency of this process and hence the output power of the generated radiation in this scheme is also less. Generation of mid-infrared radiation is also possible by second and third harmonic generations in other MIR crystals from CO_2 laser radiations having tunability of wavelength in 9–11 μm region. Second harmonic generation (SHG) of CO_2 laser radiation has been reported by several authors [1–4] and also third harmonic generations by some [5–7]. Although the region can also be covered [8] by optical parametric oscillator (OPO) in MIR crystals including $AgGaSe_2$ using ~ 2 μm as pump, the demand of very high quality crystal for OPO, being a resonant device precludes this proposition.

This is due to the considerable absorption in the pump wavelength region in our crystal (as illustrated in the figure 3). Here we report the generation of 3.53 (third harmonic of 10.6 μm) and 5.3 μm (second harmonic of 10.6 μm) radiations in AgGaSe$_2$ crystal by sum-frequency-mixing and second harmonic generation processes using the CO$_2$ laser as the fundamental radiation source at 10.6 μm. To the best of our knowledge this is the first report of the generation of third harmonic of a TEA CO$_2$ laser radiation in AgGaSe$_2$ crystal by type-II phase matching. The crystal used for third harmonic generation (THG) is a type-II, $\theta = 57°$ cut crystal whereas the one used for SHG is type-I, $\theta = 55°$ cut. The use of CO$_2$ laser radiation is advantageous due to readily available high power of the input fundamental pump laser. Moreover the pulse width of the fundamental laser radiation can be varied. We set up a CO$_2$ laser amplifier-chain to scale up the energy and power to the desired level without sacrificing the useful properties of the laser beam. Because of our two-step process for THG the prospect of higher overall non-linear conversion efficiency is low here as compared to the OPO and DFG (difference frequency generation) being single-step process. Because of the many complexities in [7], we consider [6] and our route is a useful competitive alternative to the MIR source in the region due to the availability of the well-behaved compact TEA CO$_2$ laser system.

2. CO$_2$ laser

Figure 1 shows the schematic layout of the laboratory built CO$_2$ laser. The oscillator is a hybrid configuration, consisting of a CW and a TEA (transversely excited electrical discharge at atmospheric pressure) contained in a common resonator. The gain bandwidth of TEA laser is $\sim$3 GHz broad. A large number of longitudinal modes will be operating under this condition. The CW section is operated at low pressure and has a linewidth of $\sim$60 MHz. The longitudinal mode, at the line center, experiences the maximum gain of the TEA section and also experiences the added gain of the CW section. Thus this longitudinal mode will grow at the expense of other modes. Without the CW section the temporal profile of the output pulse exhibits self mode locking and modulations on the pulse which varies with time. When the CW section is operated near threshold the output is in the form of a smooth gain switched spike followed by a tail of $\sim$800 ns width. The width (FWHM) of the spike varies from 200–220 ns. The width of the spike measured during the experiment is $\sim$216 ns and is shown in figure 2a and the spike contain about 2/3rd of the total energy. The output is quite stable as well as reproducible. Figure 1 (inset) shows the hybrid section in detail. The aperture A restricts the operation of the laser to the TEM$_{oo}$ mode. The section uses a gas mixture of CO$_2$:N$_2$:He in the ratio 1:1:4 at a total pressure of 1 atmosphere. The CW section in contrast uses a longitudinal discharge in a gas mixture of CO$_2$:N$_2$:He in the ratio 1:1:6 at a total pressure of 3 torr. The low pressure discharge tube has a ZnSe Brewster window at each end. The output beam is thus p (horizontally) polarised. The resonator consists of a fully reflective curved mirror of 5 m radius of curvature and a plane output coupler of 70% reflectivity. The maximum output energy of the oscillator is 80 mJ in the 10.6 μm $P(20)$ line. For some applications tunable source is required, for that it is necessary to replace the mirror M$_2$ by a grating. And preliminary experiments suggest that it is possible to tune the system over the CO$_2$ laser P and R branches.
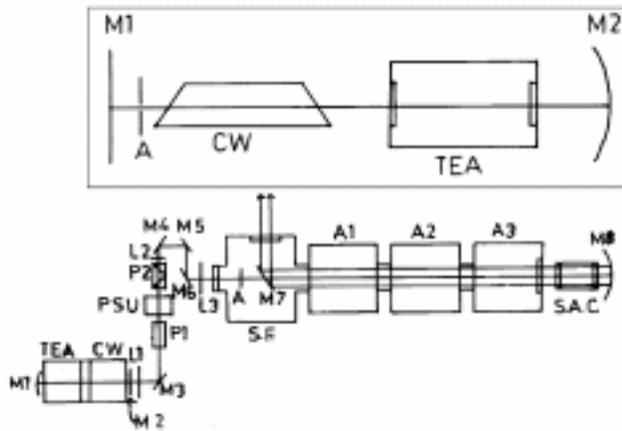
Figure 1. The schematic layout of the CO_2 laser set up, A1, A2 and A3 are three amplifier chains. M1–M8 mirrors. L1, L2 and L3 are three lenses. P1 and P2 are polarisers. Inset shows the hybrid oscillator section in detail. A is the aperture.

The linearly polarised output laser pulse from the hybrid oscillator passes through a pulse slicer unit which incorporates a CdTe Pockel cell. By choosing the length of the pulse forming cable of this unit we generate 6 ns (FWHM) laser pulse and it is shown in figure 2(b). For operation of the laser in the normal long pulse mode, the polariser P2 is made parallel to P1. In figure 1 they are shown as crossed for short pulse generation. Temporal distribution of both the long pulse and short pulse has been measured using a Photondrag detector. Due to residual birefringence of the CdTe crystal used in the Pockel cell, the short pulse is accompanied by an unavoidable background pulse of 216 ns duration. It is desirable that the output of the amplifier be free of this background pulse. A saturable absorber cell 10 cms long, filled with 1 mbar of SF_6 and 5 mbar of He is used for this purpose. The cell is used after the first pass and attenuates the background pulse in preference to the short pulse. The short pulse dominates in the return pass and the output pulse has negligible background content. SF_6 is the saturable component and He is used to improve the absorption of the long pulse CO_2 laser radiation by SF_6 [9]. Due to its narrow line-width the long pulse laser interacts with only a small number of SF_6 molecules. $HeSF_6$ collisions repopulate the absorbing state causing more absorption.

Before the laser beam enters the amplifiers it is passed through a spatial filter unit. This unit uses a lens and an aperture to allow only a gaussian beam to propagate beyond this unit. The amplifier chain consists of 3 amplifier modules. Each of these modules houses a uv pre-ionized TEA CO_2 laser discharge assembly. The discharge is 50 cm long with 3 cm square cross section. The discharge electrodes are spaced at 3 cm, thus defining the discharge height. The discharge is obtained between a Chang profiled [10] electrode and a perforated plane electrode. A flash board kept behind the perforated electrode act as the UV pre-ioniser. The flash generated by the flashboard is rich in UV. It is reported that [11] 100–200 mm wavelength region of the UV spectrum is most effective. The UV light illuminates the discharge region and produces electrons by ionization of hydrocarbon impurities in the gas mixture. The flashboard uses stainless steel discs placed over a glass
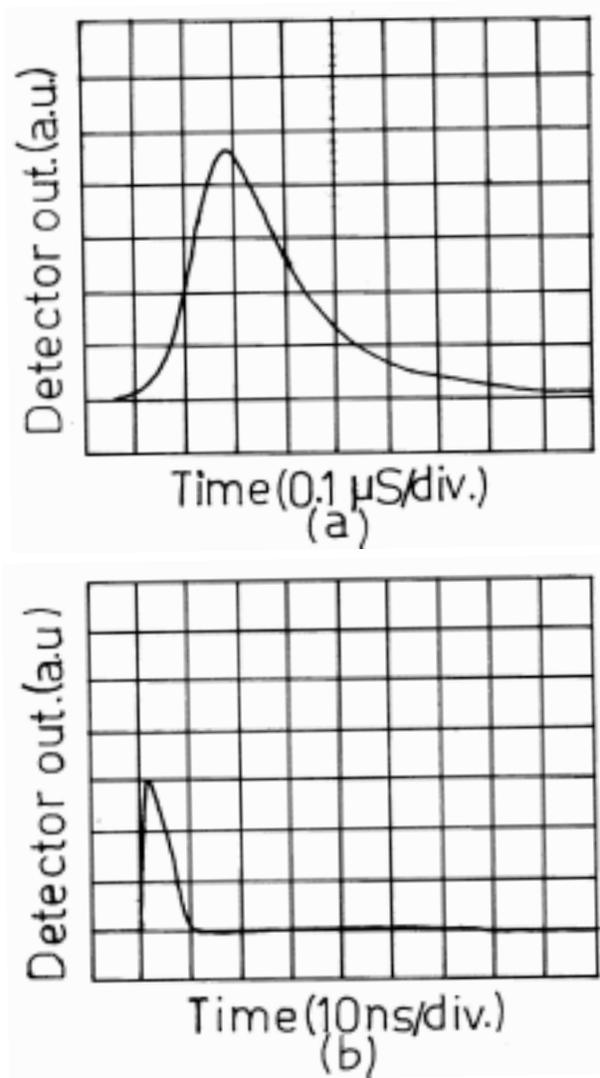
Figure 2. (**a**) The temporal distribution of energy of the TEA CO_2 laser (long) pulse used in this experiment. (**b**) The temporal distribution of energy of the TEA CO_2 laser (short) pulse used in this experiment.

plate. On application of high voltage pulse the gaps between the discs break down and a discharge occurs over the glass surface.

The diameter of the beam at the output of the hybrid oscillator is ∼8 mm. This diameter is maintained during the passage of the beam through the pockel cell by the lens L_1. Lenses L_2 and L_3 determine the propagation characteristics of the beam after the pulse slicer unit. The beam is initially focussed, reduced in diameter and is filtered by the aperture A. The beam then expands to a diameter of ∼20 mm at the end of the forward pass through the

408

amplifier, on the mirror M8. During the forward pass the expanding beam passes through a central hole of diameter 6 mm in M7, a scraper mirror. M8 is a curved mirror which collimates the return beam with a beam diameter of 20 mm. The return beam reflected by the mirror M7 serves as the useful output beam and is used in the harmonic generation experiment.

3. Experiment and results

AgGaSe$_2$ is a negatively birefringent uniaxial crystal which belongs to $\bar{4}2m$ symmetry. The crystal has wide transmission range (0.73–18.0 μm). Figure 3 shows the optical trans- mission spectra of the AgGaSe$_2$ crystal samples having thickness 9 mm (solid curve) and 11 mm (dashed curve) at room temperature. The absorption of 11 mm thick SHG crystal at 10.6 and 5.3 μm is less than 0.01 cm^{-1}. Whereas the absorption of 9 mm thick THG crystal at 10.6 μm is although less than 0.01 cm^{-1} but the absorption coefficients at 5.3 and 3.53 μm rises to $\sim$0.6 and 0.2 cm^{-1} respectively. The absorption coefficient a_i (in cm^{-1}) at different wavelength λ_i has been calculated using the following relation:

$$a_i = -(1/L) \ln[\{((1 - R_i)^4/4T_i^2 + R_i^2)^{0.5} - (1 - R_i)^2/2T_i\}/R_i^2],$$

where $R_i = [(n_i - 1)/(n_i + 1)]^2$; n_i is the equivalent refractive index given by $n_i = [n_i^e(n_i^o)^2]^{1.5}$, n_i^e and n_i^o being the refractive indices [12] of the crystal for ordinary and ex- traordinary polarised λ_i beam and L is the crystal thickness. The transmission coefficients (T_i) throughout the transmission range of the crystal have been measured using two spec- trophotometers, Hitachi (U-3400, 0.185–2.6 μm) and Shimadzu (IR-470, 2.5–25.0 μm).
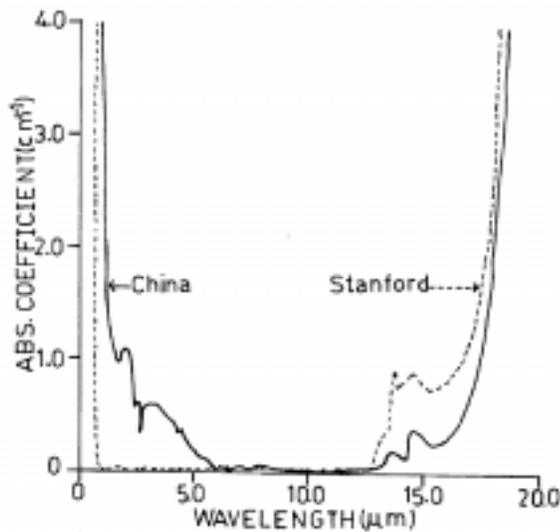

Figure 3. The optical absorption spectrum of 11 and 9 mm thick AgGaSe$_2$ crystals. The dashed curve is for 11 mm thick SHG crystal and the solid curve is for 9 mm thick THG crystal.

The experiment has been performed both with long pulse (216 ns pulse width) and short pulse (with pulse width 6 ns FWHM) mode of the CO_2 laser. The repetition rate of the laser pulse is 1 pulse per sec. The incident beam diameter coming after reflection from the mirror M7 is $\sim$20 mm. To reduce the diameter of the beam a lens of focal length 50 cm has been used before the SHG crystal in such a way that both the SHG and THG crystals are kept well away from the focus. The experiment has been done in two steps. In the first step we generate the second harmonic of 10.6 μm radiation in a type-I, $\theta = 55\,^\circ$ cut AgGaSe$_2$ crystal (thickness 11 mm). The type-I, $\theta = 55^\circ$ cut AgGaSe$_2$ crystal has been placed on a rotation table. The input fundamental beam is polarised in the horizontal plane and hence we rotate the crystal in the vertical plane to satisfy the condition for type-I phase matching $(o + o \rightarrow e)$. The calculated [12] value of the phase matching angle for second harmonic generation is 56.8° and the maximum second harmonic conversion is observed at near normal incidence of the fundamental laser beam. A 3 mm thick sapphire filter is used in front of the energy meter to separate out the second harmonic beam from the unconverted fundamental beam. And this 3 mm thickness has been found sufficient to block the residual fundamental radiation completely. The input beam intensity is varied by any of the following: By varying either the lens to crystal distance, or by using CaF$_2$ plate as attenuator, or changing the width of the laser pulse. Figure 4 shows the variation of the SHG conversion efficiency with variation of the input beam intensity. For measurement of energy of both the generated SHG and THG radiations and the fundamental radiation, a pyroelectric energy meter (Molectron make) has been used. In the process we obtain maximum energy conversion efficiency of 6.3% when the input fundamental beam intensity is 5.9 MW/cm^2 and the pulse width of the input beam is 6 ns. This is well within the safe limit for crystal damage, the quoted literature value being 10–20 MW/cm^2. With longer crystal (2–3 cm) as expected, people [1–3] reported higher SHG conversion efficiency. Here solid curve is theoretical [13]. Filled circles and the open circles are obtained experimentally when the laser has been operated in the long pulse and short pulse modes respectively. Horizontal and vertical error bars are shown to indicate the fluctuations in energy of the input parent beam and the generated beam respectively. Both the SHG and THG crystals used in the experiment are uncoated and during calculation the reflection losses of the incident energy from the crystal entrance and exit faces have been taken into account. The value of the effective non-linear coupling coefficient has been taken as $d_{36} = 33$ pm/V [2].

In the second step we remove the sapphire filter and both the second harmonic and the residual unconverted fundamental radiations are allowed to be incident on another type-II, $\theta = 57^\circ$ cut AgGaSe$_2$ crystal (thickness 9 mm) placed on a precision rotation table. We rotate the THG crystal on the horizontal plane. Therefore the polarization of the generated second harmonic beam becomes vertical with respect to the THG crystal optic axis direction and the polarization for the fundamental beam becomes horizontal. The condition for type-II $(e + o \rightarrow e)$ phase matching is thereby satisfied. A quartz filter of thickness 2 mm is used to block the third harmonic beam from its parent beams. The experimentally measured phase matching angle for THG of 10.6 μm radiation is 57° ($\pm$0.1°) which agrees quite well with the corresponding theoretical value of 57.1° [12]. The inset of figure 4 shows the variation of the generated third harmonic energy with the rotation of the crystal from the exact phase matching position. The solid curve is calculated from ref. [13] and the dots denote the experimental points. The measured value of angular phase-matching bandwidth (internal) for THG process is 1.00 deg-cm and the corresponding calculated value is 0.99 deg-cm. The energy of the generated third harmonic beam is $\sim$60 μJ which
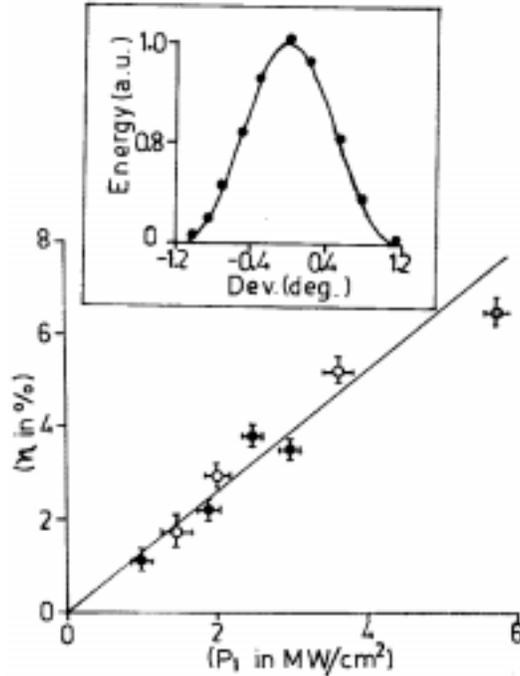
Figure 4. Variation of SHG conversion efficiency (η in %) with the pump beam intensity (P_1 in MW/cm^2) in 11 mm thick AgGaSe$_2$ crystal. The fundamental wavelength is 10.6 μm, $P(20)$ line. Filled circles ($\bullet$) and the open circles (o) are experimental points for long and short pulses, respectively. Solid curve is theoretical. The horizontal and the vertical bars have been given to show the fluctuation of the parent beam energy and that of generated beam respectively. Inset shows the variation of the relative generated energy of the third harmonic beam (in a.u.) with the angular deviation of the THG crystal from the exact phase matching position.

corresponds to an energy conversion efficiency (η) 2.4% when the energy of the input 10.6 μm and 5.3 μm beams are 6 mJ and 1.14 mJ respectively. Here we use the relation $\eta = E_3 / \sqrt{(E_1 E_2)}$ for the calculation of the conversion efficiency for THG process. E_3, E_1 and E_2 are the energies of third harmonic, incident fundamental and second harmonic beams respectively. The pulse width of the input fundamental beam is 6 ns in this case also.

An internal conversion efficiency $\sim$10% is calculated for SHG without including Fresnel reflections loss, if the front and the rear ends of the SHG crystal are anti-reflection coated at the fundamental and SHG wavelengths. Fresnel reflection loss at these wavelengths can be greatly reduced if the front face and the rear face of the THG crystal are also anti-reflection coated at 5.3, 10.6 and 3.53 μm. Hence the internal conversion efficiency $\sim$2.6% for THG is calculated without considering Fresnel reflection loss. The absorption in the THG crystal at 5.3 and 3.53 μm are 0.6 and 0.2 cm^{-1} respectively which are larger than their corresponding values for the SHG crystal (it is less than (0.01 cm^{-1})). Therefore us-

ing crystals having low absorption loss (≤ 0.01 cm^{-1}) at the three interacting wavelengths a conversion efficiency greater than 2.6% for THG can be obtained easily. Further exploiting the tunability of the CO_2 laser, the corresponding tunability can be realised thereby potentially making the system useful for detecting absorption of methane lying in this region. Finally the following comment is in order in respect of THG of CO_2 laser in a related crystal as reported recently [7].

Generation through realisation of non-critical phase matching (NCPM) in this type of negative uniaxial crystal is advantageous from device point of view, since under NCPM apart from large angular tolerance high effective non-linear coupling is realised leading to higher conversion efficiency. However, the generation of third harmonic of CO_2 laser radiation in $AgGa_xIn_{1-x}Se_2$ (a material derived and very much related to our $AgGaSe_2$ crystal) through NCPM as reported recently in [7] fails to realise and quote the achieved conversion efficiency. Though the angular acceptance bandwidth ~ 8.2 ° is higher than our value of $\sim 1°$, the advantage is overshadowed by the critical requirements of maintenance of crystal compositional parameter x to an accuracy within 1% with subsequent requirement of temperature tunability to compensate for such inaccuracy in x.

Acknowledgement

References

[1] R C Eckardt, Y X Fan, R L Byer, R K Route, R S Feigelson and Jan van der Laan, *Appl. Phys. Lett.* **47**, 786 (1985)

[2] R L Byer, M M Choy, R L Herbst, D S Chemla and R S Fiegelson, *Appl. Phys. Lett.* **24**, 65 (1974)

[3] G W Iseler, Y X Fan and N Menyuk, *Inst. Phys. Conf. Ser.* **24**, 73 (1977)

[4] G C Bhar, S Das, U Chaterjee, A M Rudra, R K Route and R S Feigelson, *J. Appl. Phys.* **74**, 5282 (1993)

[5] A Rosengreen, J E van der Laan, E R Murray and L L Alpeter, *Proceedings on the Workshop for gas distribution and safety instrumentation* (Orlando, Florida, 1983) Feb. 1–3

[6] G C Catella and D Burlage, *Materials Research Society Bulletin (USA)* **23(7)**, 28 (1998)

[7] Eiko Takaoka and Kiyoshi Kato, *Opt. Lett.* **24**, 902 (1999)

[8] C L Marquardt, D G Cooper, P A Budni, M G Knights, K L Schepler, R DeDomenico and G C Catella, *Appl. Opt.* **33**, 3192 (1994)

[9] R F Haglund, A V Nowak and Stephen J Czucchlewski, *IEEE J. Quantum Electron* **QE-17(9)**, 1799 (1981)

[10] T Y Chang, *Rev. Sci. Instrum.* **44**, 405 (1973)

[11] H J Seguin, D McKen and J Tulip, *IEEE J. Quantum Electron.* **QE-11**, 710 (1975)

[12] G C Bhar, *Appl. Opt.* **15**, 305 (1976)

[13] F Zernike, *Methods of experimental physics* part B, edited by C L Tang (Academic Press, New York, 1979) vol. 15, pp. 143–183